MOLECULAR AND CELLULAR BIOLOGY, Dec. 1988, p. 5398–5409
0270-7306/88/125398-12$02.00/0

Vol. 8, No. 12

Matrix Attachment Regions Are Positioned Near Replication Initiation Sites, Genes, and an Interamplicon Junction in the Amplified Dihydrofolate Reductase Domain of Chinese Hamster Ovary Cells

PIETER A. DIJKWEL AND JOYCE L. HAMLIN*

Department of Biochemistry and Cell and Molecular Biology Program, University of Virginia School of Medicine, Charlottesville, Virginia 22908

Received 23 June 1988/Accepted 23 September 1988

Genomic DNA in higher eucaryotic cells is organized into a series of loops, each of which may be affixed at its base to the nuclear matrix via a specific matrix attachment region (MAR). In this report, we describe the distribution of MARs within the amplified dihydrofolate reductase (DHFR) domain (amplicon) in the methotrexate-resistant CHO cell line CHOC 400. In one experimental protocol, matrix-attached and loop DNA fractions were prepared from matrix-halo structures by restriction digestion and were analyzed for the distribution of amplicon sequences between the two fractions. A second, in vitro method involved the specific binding to the matrix of cloned DNA fragments from the amplicon. Both methods of analysis detected a MAR in the replication initiation locus that we have previously defined in the DHFR amplicon, as well as in the 5′-flanking region of the DHFR gene. The first of these methods also suggests the presence of a MAR in a region mapping ~120 kilobases upstream from the DHFR gene. Each of these MARs was detected regardless of whether the matrix-halo structures were prepared by the high-salt or the lithium 3,5-diiodosalicylate extraction protocols, arguing against their artifactual association with the proteinaceous scaffolding of the nucleus during isolation procedures. However, the in vitro binding assay did not detect the MAR located 120 kilobases upstream from the DHFR gene but did detect specific matrix attachment of a sequence near the junction between amplicons. The results of these experiments suggest that (i) MARs can occur next to different functional elements in the genome, with the result that a DNA loop formed between two MARs can be smaller than a replicon; and (ii) different methods of analysis detect a somewhat different spectrum of matrix-attached DNA fragments.

In the eucaryotic genome, the chromatin loop represents a basic structural unit. The loops are generated by periodic attachment of the chromatin fiber to a nonhistone chromosomal protein scaffolding in the nucleus, which has been referred to as the nuclear matrix (3, 8, 9, 36). During mitosis, part of this matrix probably rearranges to become the metaphase chromosomal scaffold (2, 19). Although neither the interphase nuclear matrix nor the mitotic chromosomal scaffold has been fully characterized as yet, topoisomerase II has been identified as an integral component of both (5, 14). This finding has led to the suggestion that the nuclear matrix may somehow poise individual chromatin domains for transcription by allowing torsional stress to be introduced into defined regions (7). Nonrandom organization of the chromatin is further suggested by the presence at the base of the loops of specific DNA sequences that associate with the nuclear matrix. In *Drosophila* cells, specific matrix attachment regions (MARs) have been found in the 5′-flanking regions of several active genes (12, 26, 33), and these MARs coincide with enhancerlike elements (12). However, in the murine κ light-chain gene, an attachment site is found at an intragenic site close to, but separable from, the enhancer (7). An intragenic MAR has also recently been described in the Chinese hamster dihydrofolate reductase (DHFR) gene (19). Virtually every MAR that has been sequenced, whether from *Drosophila* or mammalian cells, contains a topoisomerase II consensus sequence (7, 13, 19). These findings again suggest a role for this enzyme in higher-order chromatin organization.

Other functional approaches suggest that the matrix is involved in DNA replication (4, 9, 36), and it is conceivable that the replication machinery is actually affixed to the matrix. Interestingly, estimates for the average size of looped domains are quite similar to size estimates for eucaryotic replicons (6, 36), so that each loop might be equivalent to a replicon containing one origin of DNA synthesis. In addition, several studies suggest that origins may remain attached to the matrix throughout the cell cycle (10, 30, 35). It has also been proposed that DNA sequence amplification may involve the overreplication and subsequent integration into the chromosome of one or more chromosomal loops (15, 32).

Thus, there is considerable evidence that the nuclear matrix plays an important role in the structural organization of chromatin, and it is likely that attachment of DNA to the matrix facilitates both transcription and replication processes. However, a clear picture of the overall structure of a single functional unit in the mammalian chromosome is lacking.

In this study, we have begun to analyze the spatial organization of the amplified DHFR domain (amplicon) in the nucleus of a well-characterized methotrexate-resistant Chinese hamster ovary cell line (CHOC 400). The CHOC 400 cell line contains approximately 1,000 DHFR amplicons, which are carried in three stable chromosomal locations (one major and two minor sites) (25). We have recently isolated

* Corresponding author.

the equivalent of two complete amplicon types from CHOC 400 cells by molecular cloning in overlapping cosmids (22) (see Fig. 1). Several functional sequences have been identified within the DHFR amplicon in addition to the interamplicon junction fragments that define the boundaries of the type I and II sequences. For example, there are at least two other transcription units in this locus that are distinct from the DHFR gene itself (27; P. Foreman and J. L. Hamlin, submitted for publication). One of these additional genes appears to begin transcription at a site within the DHFR promoter but is transcribed in the opposite direction (27). We have also shown that replication in the DHFR domain initiates somewhere within a 28-kilobase (kb) locus mapping downstream from the DHFR gene (16) and have recently obtained evidence that there may actually be two closely spaced initiation sites within this locus (T.-H. Leu and J. L. Hamlin, submitted for publication) (Fig. 1A).

Thus, the major amplicon type in CHOC 400 cells probably contains at least one complete functional chromosomal unit, since two replication initiation sites have been identified in this domain in addition to at least three active genes. The system therefore provides a unique opportunity to analyze the spatial organization of a large, defined sequence in the nucleus. In the studies described in this report, we scanned the entire amplified sequence by using two separate experimental approaches and have identified several specific matrix attachment sites; these occur close to the replication initiation sites, in the 5′-flanking region of the DHFR gene, and near an interamplicon junction.

MATERIALS AND METHODS

Cell culture and labeling protocols. Parental CHO cells and the methotrexate-resistant derivative, CHOC 400, were grown as monolayers in 15-cm dishes on minimal essential medium as previously described (25). The CHOC 400 cell line was maintained in 0.8 mM methotrexate (obtained from the National Cancer Institute, Drug Development Branch). Matrices were prepared from subconfluent cultures (five plates per sample), to one of which was added 0.5 μCi of [^{3}H]thymidine per ml (80 Ci/mmol; Dupont-NEN Research Products) for at least 16 h in order to trace label the DNA. All tissue culture media, sera, etc., were obtained from GIBCO Laboratories.

Nuclear matrix isolation. For the preparation of high-salt matrices (3, 9), ~10^8 cells (five 15-cm plates) were trypsinized, pooled, collected by centrifugation, and washed with fresh medium containing 10% donor calf serum to neutralize any remaining traces of trypsin. All subsequent steps were performed in a cold room. The cells were washed twice in 50 mM KCl–5 mM Tris hydrochloride (pH 7.4) (KT buffer) and were suspended in KT buffer containing 0.5% Triton X-100. The suspension of swollen cells was then forced four times through a 21-gauge hypodermic needle. Nuclei were collected by centrifugation, washed once with KT-Triton buffer, and suspended in KT buffer containing 10 mM $MgCl_2$. All of the above washing and lysis steps were carried out in a volume of 10 ml per plate equivalent of cells (~2×10^7), and centrifugations were performed in an International Equipment Co. benchtop clinical centrifuge for 5 min at a setting of 4. After the KT buffer wash, an equal volume of 4 M NaCl was added to the nuclear suspension, and after allowing extraction to proceed for 10 min, matrices were collected by centrifugation in a Sorvall HB-4 rotor for 20 min at 7,000 rpm. Finally, the matrix-halo pellet was washed twice in the HB-4 rotor for 5 min at 7,000 rpm with the appropriate restriction buffer, and the matrices were suspended in 7.5 ml of restriction buffer.

Alternatively, matrices were prepared by a modification of the lithium 3,5-diiodosalicylate (LIS) extraction method of Mirkovitch et al. (26). The cells (~10^8) were trypsinized, washed once with fresh medium containing serum and twice with cold cell wash buffer (CWB; 50 mM KCl, 0.5 mM EDTA, 0.05 mM spermine, 0.125 mM spermidine, 0.5% thiodiglycol, 0.25 mM phenylmethylsulfonyl fluoride, 5 mM Tris hydrochloride, pH 7.4). Cell lysis was effected by suspending the pellets in cold CWB containing 0.1% digitonin (2×10^7 cells per 5 ml) and forcing the suspension twice through a 21-gauge needle. The nuclear suspension (10 ml) was layered over 5 ml of 10% glycerol in CWB-digitonin, and nuclei were pelleted in a benchtop centrifuge at a setting of 4 for 10 min at 4°C. The pellets were then washed once with 10 ml of cold CWB–0.1% digitonin, and 10^8 nuclei were suspended in 5 ml of stabilization buffer (CWB in which 0.5 mM EDTA was replaced by 0.5 mM $CuSO_4$ and to which 0.1% digitonin was added). After incubation for 20 min at 37°C, nuclei were extracted for 10 min with 19 volumes of room temperature LIS buffer (10 mM LIS, 100 mM LiAc, 0.1% digitonin, 0.05 mM spermine, 0.125 mM spermidine, 0.25 mM phenylmethylsulfonyl fluoride, 20 mM HEPES [*N*-2-hydroxyethylpiperazine-*N*′-2-ethanesulfonic acid]-potassium hydroxide, pH 7.4; total volume, approximately 100 ml/10^8 cells). Matrices were collected by centrifugation (20 min at 4,000 rpm in the HB-4 rotor at 20°C) and were washed once in matrix wash buffer (20 mM KCl, 70 mM NaCl, 10 mM $MgCl_2$, 20 mM Tris hydrochloride, pH 7.4) containing 0.1% digitonin and then washed twice with matrix wash buffer and once with the appropriate restriction buffer at 20°C. The preparation of nuclei was monitored by phase-contrast microscopy. Nuclear matrix preparations were examined by fluorescence microscopy for characteristic matrix-halo structures after the DNA was stained with 4 μg of ethidium bromide per ml (36).

Isolation and analysis of matrix-attached DNA (MAD). Matrices were digested with restriction enzymes (alone or in combination) for a total of 3 h at 37°C in the buffers recommended by the supplier (Bethesda Research Laboratories; 40 U of enzyme per ml; ~10^8 nuclear equivalents per 7.5 ml). After 90 min of digestion, matrices were collected by centrifugation in an HB-4 rotor for 10 min at 20°C (7,000 rpm for high-salt matrices and 4,000 rpm for LIS matrices), suspended in 5 ml of restriction buffer, and digested with 50 U of fresh restriction enzyme(s) per ml for an additional 90 min. Digestion was stopped by adding EDTA to a concentration of 25 mM. An equal volume of either 4 M NaCl or 10 mM LIS buffer was added, and the matrices were collected by centrifugation in the HB-4 rotor at 5,000 rpm for 20 min at 20°C. The pellet from 10^8 cells was washed at room temperature in matrix wash buffer containing 1 mM EDTA instead of $MgCl_2$ and was then dissolved in 1 ml of 1% sodium dodecyl sulfate (SDS)–10 mM Tris hydrochloride–1 mM EDTA, pH 7.4. DNA detached from the matrices by the action of the restriction enzyme(s) (termed loop DNA) was collected by precipitation of the supernatant (including the wash) with 2 volumes of cold absolute ethanol. After 16 h at −20°C, the precipitate was pelleted by centrifugation in the cold and suspended in 1 ml of 10 mM Tris hydrochloride–1 mM EDTA, pH 7.4.

Both MAD and loop DNA fractions were incubated with 200 μg of Proteinase K (Boehringer Mannheim) per ml and 1% SDS for 4 h at 50°C or for 8 h at 37°C. They were then extracted twice with phenol-chloroform and were ethanol

precipitated twice (after the addition of NaCl to a concentration of 100 mM and $MgCl_2$ to a concentration of 10 mM). Finally, DNA was dissolved at an appropriate concentration in 10 mM Tris hydrochloride–1 mM EDTA, pH 7.4.

The relative amount of DNA remaining attached to the matrix after digestion was estimated by determining the proportion of acid-precipitable [^{3}H]thymidine in this fraction relative to the total amount of label in the matrix preparation prior to digestion. DNA concentrations were additionally determined by a fluorimetric assay based on Hoechst staining (20). In a typical matrix preparation digested with an enzyme such as *Eco*RI, 4% of the total DNA remains attached to the matrix, which is close to the figure one would expect if the enzyme cuts every 4 kb on average and if chromosomal loops are 80 to 100 kb in length (6, 21, 36). Incubation with the combination *Eco*RI-*Hin*dIII-*Bam*HI-*Pvu*II reduced this proportion to 1 to 2%.

MAD and loop DNA fractions were analyzed by Southern blotting and hybridization procedures in order to determine the distribution of amplicon sequences between the two fractions. In the first approach, restriction digests of a series of 10 recombinant cosmids that span the entire 273-kb type I DHFR amplicon (500 ng each) were separated on agarose gels and were transferred to GeneScreen Plus (Dupont-NEN Research Products) after acid depurination according to the recommendation of the supplier (Dupont-NEN brochure NEF-976). The transfers were then probed with MAD or loop fractions (~50 ng) that were labeled in vitro with [^{32}P]dCTP by the random primer method (11). Hybridization was performed in 50% formamide–10% dextran sulfate–1 M NaCl–1% SDS at 42°C for 24 to 48 h. In most experiments (see figure legends), sonicated CHO genomic DNA was added to each probe before boiling and addition to the hybridization solution (50 to 100 μg of final concentration per ml in the bag). The transfers were washed twice at room temperature in 2× SSC (1× SSC is 0.15 M NaCl plus 0.015 M sodium citrate, pH 7.0), twice for 30 min at 65°C in 2× SSC–1% SDS, once for 30 min at 65°C in 0.2× SSC-1% SDS, and once for 30 min at room temperature in 0.1× SSC. The filters were placed next to Kodak X-Omat film and an intensifying screen at −70°C. In some experiments, the filters were stripped of the previous probe according to the procedure described in Dupont-NEN bulletin NEF-976. They were then reprobed as described above.

In a second approach, 1 μg each of the MAD and loop DNA fractions were separated as pairs on a 1% agarose gel. The DNA was transferred to GeneScreen Plus as above, and the transfer was cut into strips containing a pair of digests. Each strip was then probed with one of the series of ten recombinant cosmids that had been labeled with [^{32}P]dCTP by the random primer method (11). Hybridization and washing were performed as described above.

In some experiments, single restriction fragments to be used as probes were excised from an appropriate cosmid digest separated on a low-melting-point agarose gel (Bethesda Research Laboratories, Inc.). The fragment in the agarose was then labeled by random priming (11).] Most probes were in the range of 0.5×10^9 to 1×10^9 cpm/μg of DNA.

In vitro binding assay. The affinity of specific amplicon sequences for the nuclear matrix was determined by a modification of the approach described by Gasser and Laemmli (12). Matrix-halo preparations were isolated from parental, drug-sensitive CHO cells by the LIS method as described above. Preparations from 10^7 nuclei were suspended in 300 μl of *Hin*dIII buffer, and to each 300-μl sample was added 0.25 to 1.0 μg of a *Hin*dIII digest of a cosmid from the amplicon (similar results were obtained if undigested cosmids were added at this stage). Approximately 75 U of the appropriate restriction enzyme(s) was added to the matrix-cosmid mixtures, and digestion proceeded for 3 h at 37°C. The reaction was stopped by adding EDTA to a concentration of 25 mM, after which the volume was adjusted to 750 μl and an equal volume of LIS extraction buffer was added. Matrices were then collected by centrifugation and were washed once in restriction buffer (25 mM EDTA instead of $MgCl_2$) and once in 10 mM Tris hydrochloride–1 mM EDTA, pH 7.4. The MAD fraction was isolated, purified, and separated on agarose gels. After transfer to GeneScreen Plus, the digests were probed with ^{32}P-labeled cosmids in the presence of 50 μg of CHO DNA per ml of hybridization buffer.

RESULTS

Organization of DHFR amplicons in CHOC 400 cells. Figure 1A shows the series of cosmids that were used in this study. These cosmids represent two different amplicon types from the CHOC 400 genome whose structures we have defined relatively completely (22) and are part of a larger collection of overlapping amplicon clones that were isolated from CHOC 400 cells in two previous studies (22, 28). The type I amplicon, which is a minor type in this cell line (~5%), is 273 kb in length and represents a nonrearranged version of the corresponding sequence in parental CHO cells (24). The type I sequence is defined by the cosmid series extending from one end of the linear scale to the other but excludes the sequences represented by the hairpins in cosmids NQ7 and HDZ23 (see below). The multiple copies of the type I amplicon are arranged head to tail in the genome, and the map is therefore circularly permuted, beginning and ending at the interamplicon junction indicated by the interruptions in cosmids PA36 and BP22 (Fig. 1).

The major type II amplicon, which represents 75 to 80% of all amplicons in the CHOC 400 genome, is 240 kb in length and arose from the type I sequence relatively early during the amplification process by a complex rearrangement. A 33-kb region of DNA was deleted from the type I sequence (Fig. 1B, hatched areas), and a new unit of amplification was established that begins in the cosmid HDZ23 (the head), crosses the type I junction in BP22/PA36, and extends to the hairpin in cosmid NQ7 (the tail). The multiple copies of this amplicon are organized into alternating head-to-head and tail-to-tail arrays to form giant palindromes in the genome (Fig. 1B) (22).

Scanning the amplified DHFR domain for MARs. MARs are operationally defined as those sequences that remain associated with the proteinaceous scaffolding after extensive digestion of a matrix-DNA halo preparation with an endonuclease (hereafter referred to as the MAD fraction). If a specific MAR (e.g., near the 5′ end of a gene) were permanently associated with the matrix in every cell in the population, then the DNA released from the matrix-halo preparation by the action of the endonuclease (the loop fraction) would be quantitatively depleted of that specific MAR and the MAD fraction would be correspondingly enriched.

In the initial phases of the present study, our aim was to identify all of the MARs within the amplified DHFR domain without making assumptions about their possible locations. In order to screen the amplicon, we took advantage of the high copy number of the amplified DHFR domain in the CHOC 400 cell line (~1,000 per diploid nucleus) by using the

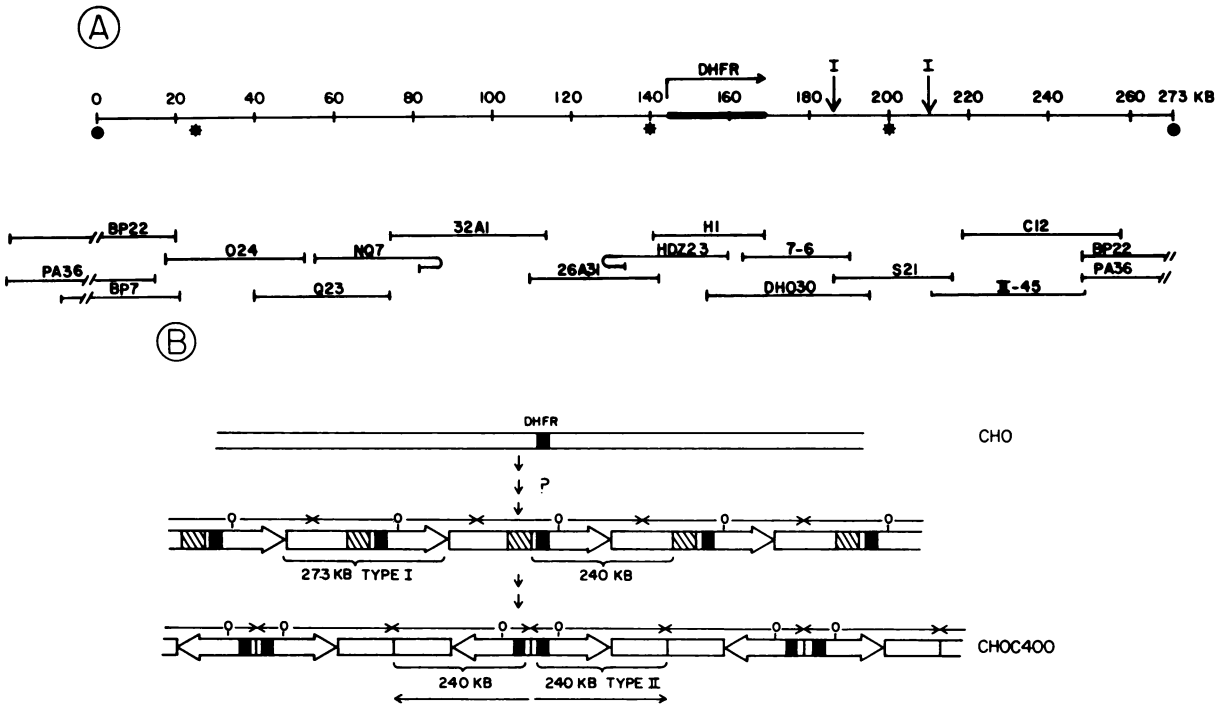

FIG. 1. Map of the amplified DHFR domain in CHOC 400 cells. (A) The linear scale is the length of the 273-kb type I amplicon, which is represented by the series of overlapping cosmids shown below (with the exception of the hairpins in the cosmids NQ7 and HDZ23, which are unique to the type II amplicon [see below]). The breakpoints in BP22 and PA36 represent the junctions between the type I amplicons, which are arranged head to tail in the genome; the map of the type I sequence is therefore circularly permuted. The type II amplicon is 240 kb long, the multiple copies are organized into head-to-head and tail-to-tail arrays in the genome, and this amplicon extends from the hairpin (junction) in HDZ23, across the type I junction in BP22, and ends at the hairpin (junction) in NQ7. The two replication initiation sites are each indicated (I) above the line. The asterisks below the scale mark the positions of MARs that were detected by two different experimental procedures (see text), while the black dots mark the MAR in PA36, which was detected by only one method. The position and direction of transcription of the DHFR gene are indicated. (B) The possible rearrangements that gave rise to the type I and II amplicons are illustrated schematically. The type I amplicon represents an early type whose internal sequences are identical to the parental CHO DHFR locus. A 33-kb internal deletion (▨) then occurred, and a new 240-kb unit of amplification with different endpoints was formed. These type II amplicons are organized into head-to-head and tail-to-tail arrays in the genome. Note that the two closely spaced replication initiation sites are indicated by a single O in the panel B. The question mark indicates that the number of rearrangements that took place to form these two amplicon types is unknown.

loop and MAD fractions themselves as probes on digests of the ordered series of cosmids and investigated whether any sequences were retained preferentially by the matrix.

Matrix-halo structures were isolated from nuclear preparations of CHOC 400 cells by modified 2 M NaCl (3) or modified LIS (26) extraction procedures. The DNA loops were then trimmed from the proteinaceous scaffolding with *Eco*RI, and the purified MAD and loop fractions were labeled in vitro with [^{32}P]dCTP and were used individually to probe transfers of *Eco*RI digests of the cosmid series shown in Fig. 1A. Hybridization was carried out in the presence of a 10^4-fold excess (wt/wt) of unlabeled CHO DNA relative to the labeled probe in order to suppress hybridization due to repetitive sequences in the genome that might partition randomly between the MAD and loop fractions.

A comparison of the signals obtained with the two probes prepared from matrices isolated by the 2 M NaCl method (Fig. 2) indicates that the MAD probe hybridizes preferentially to a 14-kb fragment in the cosmid O24, to 6.7- and 4.5-kb fragments in HDZ23, to an 11.5-kb fragment in S21, and to a 7.5-kb fragment in C12. As shown in Fig. 1A, HDZ23 contains the 5′ end of the gene as well as the head-to-head junction between the type II amplicons, and S21 is centered over the region that contains the two replication initiation sites in the DHFR domain.

From the data presented in Fig. 2, it is obvious that larger *Eco*RI fragments are preferentially retained in the MAD fraction. This result could be the consequence of preferential loss from the MAD fraction of small fragments by sliding on the proteinaceous matrix, which has been postulated to occur during extraction of histones from nuclei in high-ionic-strength buffers (26). However, when matrices were prepared in isotonic LIS instead of 2 M NaCl, the MAD fraction was not enriched for additional MARs residing in small restriction fragments. In fact, even though the 14- and 11.5-kb fragments from O24 and S21, respectively, were still enriched in the MAD fraction, the 7.5-kb fragment from the cosmid C12 was somewhat depleted, and no enrichment of the sequences contained in the cosmid BP22 was observed (data not shown; Fig. 3).

We also investigated whether the 14- and 11.5-kb *Eco*RI fragments from cosmids O24 and S21 are specifically retained in the MAD fraction because of size-dependent entrapment. Matrices were prepared in LIS and were digested with a combination of *Eco*RI, *Hin*dIII, *Bam*HI, and *Pvu*II in order to reduce the average size of the fragments remaining with the matrix (with this combination, only 1 to 2% of the total genomic DNA remains with the matrix fraction, compared with ~4% when matrix-halo structures are digested with a single enzyme).

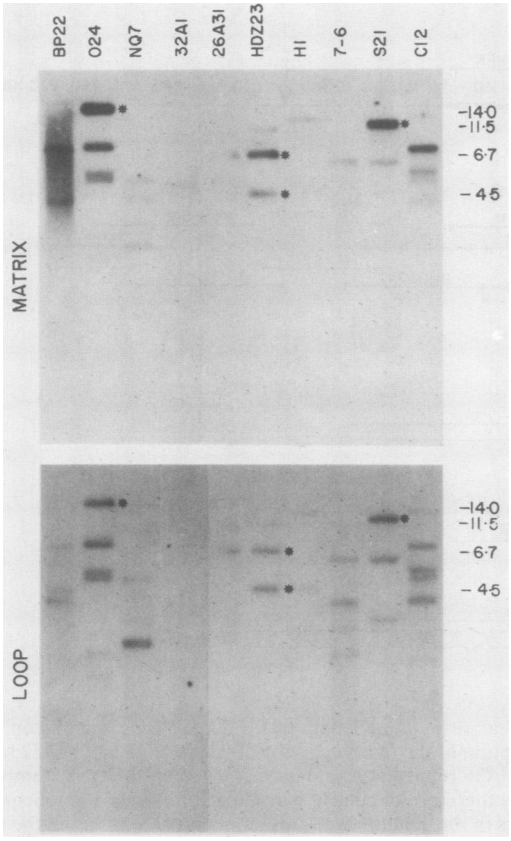

FIG. 2. Matrix-attached DNA in CHOC 400 cells is enriched for a subset of DHFR amplicon sequences. Nuclear matrix-halo structures were obtained from CHOC 400 cells by the 2 M NaCl extraction procedure and were digested with *Eco*RI. The MAD and loop fractions were isolated, labeled in vitro with [^{32}P]dCTP, and used individually to probe transfers of *Eco*RI digests of the cosmid series shown, which span the amplicon. The hybridization solution additionally contained 100 μg of parental, unlabeled CHO DNA to suppress hybridization by repetitive elements in the radioactive genomic probes. Those fragments that hybridize preferentially with the MAD probe are indicated with asterisks on both transfers in order to aid comparison. Numbers on the right indicate sizes in kilobases.

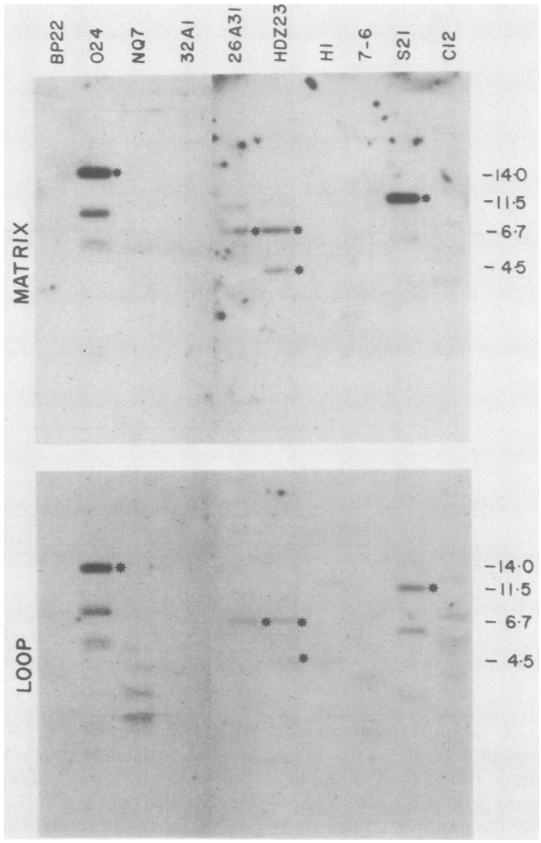

FIG. 3. Association of specific amplicon sequences with the MAD fraction is also detected in LIS-extracted matrices and does not depend on fragment size. Matrix-halo structures were prepared from CHOC 400 nuclei by extraction with 10 mM LIS and were digested with the enzyme combination *Eco*RI-*Hin*dIII-*Bam*HI-*Pvu*-II. The resulting MAD and loop fractions were radiolabeled in vitro and were used individually to probe transfers of *Eco*RI digests of cosmids in the presence of 100 μg of CHO DNA per ml. The MARs are indicated with asterisks, and their sizes (in kilobases) are shown to the right.

The hybridization patterns obtained from *Eco*RI digests of the cosmid series again show that the MAD fraction, even though reduced in size, preferentially hybridized to the 14-kb *Eco*RI fragment in O24 and very prominently hybridized to the 11.5-kb fragment in S21 (Fig. 3). In addition, the MAD fraction appeared to be somewhat enriched for the 9-kb fragment in O24 as well as the 6.7- and 4.5-kb fragments in HDZ23. Note that the 6.7-kb fragment is shared by both HDZ23 and 26A31 and was detected by the MAD probe in both cosmids (Fig. 3, upper panel). From the similarity of the hybridization patterns obtained with MAD probes from matrix-halo structures digested with *Eco*RI or with the combination of four different enzymes, we tentatively conclude that fragment size alone cannot account for the enrichment in the MAD fraction of specific amplicon sequences.

Mapping of MARs in the DHFR amplicon. While useful for scanning the large DHFR amplicon, the method used above to search for possible MARs has several drawbacks. First, it is possible that certain amplicon sequences represented in the recombinant cosmids cross-hybridize with MARs in the genomic probe that are derived from elsewhere in the genome but whose cross-hybridizing counterpart in the amplicon is not actually attached to the matrix. While a correction can be made for this phenomenon by the inclusion of competitor CHO genomic DNA along with the DNA probe, ambiguities could still arise. Second, it is not possible to estimate the actual percent enrichment of specific DNA sequences in the MAD fraction by this method, since the in vitro labeling of MAD and loop fractions is performed separately and the hybridizations necessarily have to be done in separate bags, which could lead to artifactual differences between the two samples.

We therefore analyzed the distribution of amplicon sequences between the MAD and loop fractions by the more standard method, in which equal amounts by weight of MAD and loop DNA were separated side by side on a gel and the pair was then hybridized with an individual probe (in this case, one of the cosmids shown in Fig. 1A). Competitor CHO DNA was omitted, since this method of analysis distinguishes between amplicon MARs and MARs originating from elsewhere in the genome, even if both contain repeated sequences (a given MAR in the amplicon will reside in a particular restriction fragment, which because of its high copy number will be distinguishable above any uniform

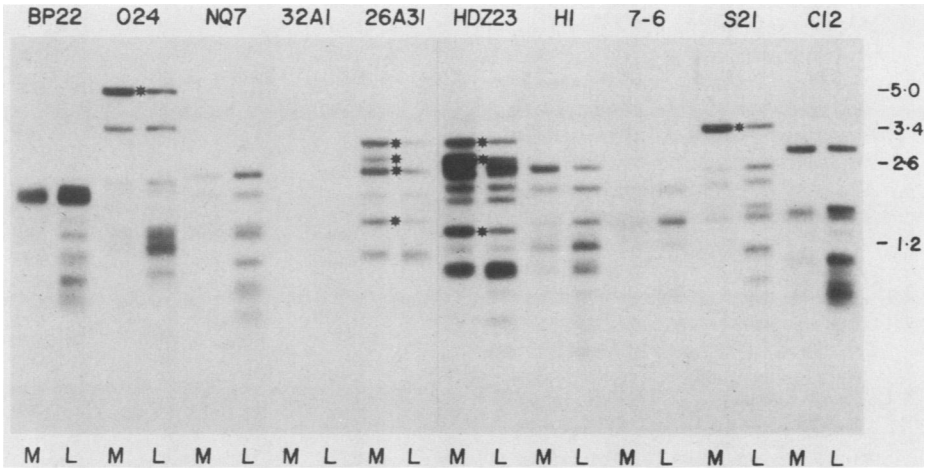

FIG. 4. The DHFR amplicon contains at least three specific MARs. LIS-extracted CHOC 400 nuclei were digested with the enzyme combination *Eco*RI-*Hin*dIII-*Bam*HI-*Pvu*II, and 1 μg each of the MAD and loop fractions were separated as pairs on an agarose gel. After transfer, the membrane was cut into strips containing a MAD and loop pair, and each strip was probed with one of the indicated radiolabeled cosmids in the absence of competitor CHO DNA. MAD and loop fractions are labeled M and L, respectively. MAD-enriched fragments are denoted with asterisks, and size markers are shown (in kilobases) to the right.

background due to other nonamplicon MARs distributed evenly over the lane).

Matrix-halo structures were prepared by the LIS method, and MAD and loop fractions were obtained with the enzyme combination *Eco*RI-*Hin*dIII-*Bam*HI-*Pvu*II. The results of this experiment are shown in Fig. 4 and essentially confirm those obtained with the alternative screening method outlined above. A 5.0-kb fragment in O24 is quite prevalent in the MAD fraction (~2.9-fold enrichment relative to loop DNA). Also, several fragments from HDZ23, which contains the 5′ end of the DHFR gene and an interamplicon junction, are enriched to varying degrees (note that several MAD-enriched fragments from HDZ23 are shared with the cosmids H1 and 26A31) (Fig. 1A). One of these (a 2.8-kb fragment that is the largest of a group of four closely spaced fragments) was sometimes found to be as much as sixfold enriched in the MAD fraction. Finally, a 3.4-kb fragment from S21, which contains the replication initiation locus in the DHFR domain, is fivefold enriched in the MAD fraction relative to loop DNA.

A MAR exists in the replication initiation locus in the DHFR domain. We have previously defined the replication initiation locus in the amplified DHFR domain by labeling CHOC 400 cells in vivo with [^{14}C]thymidine at the very beginning of the S period and analyzing the labeling pattern of the amplified restriction fragments after separation on an agarose gel (16). The most prominently labeled *Eco*RI fragments in the amplicon were a 6.2-6.1-kb doublet and an 11.5-kb fragment. These fragments (as well as two smaller ones mapping between them) defined a 28-kb initiation locus that maps downstream from the DHFR gene (17) (Fig. 1A and 5B). More recently, we have obtained evidence that replication may initiate at two distinct sites which are spaced ~22 kb apart within this locus and which map approximately at the two ends of the cosmid S21 (Leu and Hamlin, submitted) (Fig. 1A and 5B, asterisks).

To more precisely determine the position of the MAR that was identified above in S21 relative to the two initiation sites, several different restriction fragments from S21 were used to probe equal amounts of MAD and loop DNA that had been prepared from LIS matrices digested to completion with the enzyme combination *Eco*RI-*Hin*dIII-*Bam*HI-*Pvu*II. The resulting autoradiograph in Fig. 5A shows that when S21 was used as a probe (leftmost lane), a 3.4-kb fragment was preferentially retained in the MAD fraction, confirming the results of the previous experiments (Fig. 3B and 4). Since this 3.4-kb fragment was recognized by both the 6.4-kb *Hin*dIII fragment (H6.4) and the 5.4-kb *Xba*I fragment (X5.4) and since it was the only 3.4-kb *Pvu*II fragment in this region, the MAR must be located in the left half of the 11.5-kb *Eco*RI fragment (Fig. 5B).

We determined the enrichment of this element in the MAD fraction by comparing its distribution in MAD and loop and total genomic DNA relative to a second neighboring fragment (Fig. 6). LIS matrix-halo structures were digested with the enzyme combination *Eco*RI-*Hin*dIII (Fig. 6A) or *Eco*RI-*Pvu*II (Fig. 6B), and the MAD and loop and total DNA fractions were probed with the 11.5-kb *Eco*RI fragment (Fig. 5B). The results again show that the MAR in this region is localized within the 6.4-kb *Eco*RI-*Hin*dIII fragment (Fig. 6A), and the *Eco*RI-*Pvu*II digest further localizes the MAR to the 3.4-kb *Pvu*II fragment (Fig. 5B). Figure 6B also shows that while the 3.4-kb *Pvu*II fragment was clearly enriched in the MAD fraction compared with loop and total DNA, the 4.1-kb fragment was markedly depleted. This observation therefore excludes size-dependent retention as the explanation for the enrichment observed and further confirms the presence of a MAR in the 3.4-kb *Pvu*II fragment from S21. (Note that in both of these digests, there are several small fragments that are detectable on the original film but which are not detectable in the photograph. All of these appear to be present in the loop fraction only.)

From the relative intensities of the 3.4-kb *Pvu*II fragment in the MAD, loop, and total DNA fractions (Fig. 6B), the proportion of this fragment remaining associated with the matrix after LIS extraction and digestion with restriction enzymes can be roughly estimated by the equation $x/a = (I_m/I_l) \cdot [1 - x)/(1 - a)]$, where x is the fraction of fragment in the MAD fraction, a is the fraction of DNA in the matrix fraction, I_m is the relative signal of the fragment in the MAD fraction, and I_l is the relative signal of the fragment in the loop fraction.

Since about 98% of the DNA in the matrix-halo preparation was solubilized by digestion with the four restriction

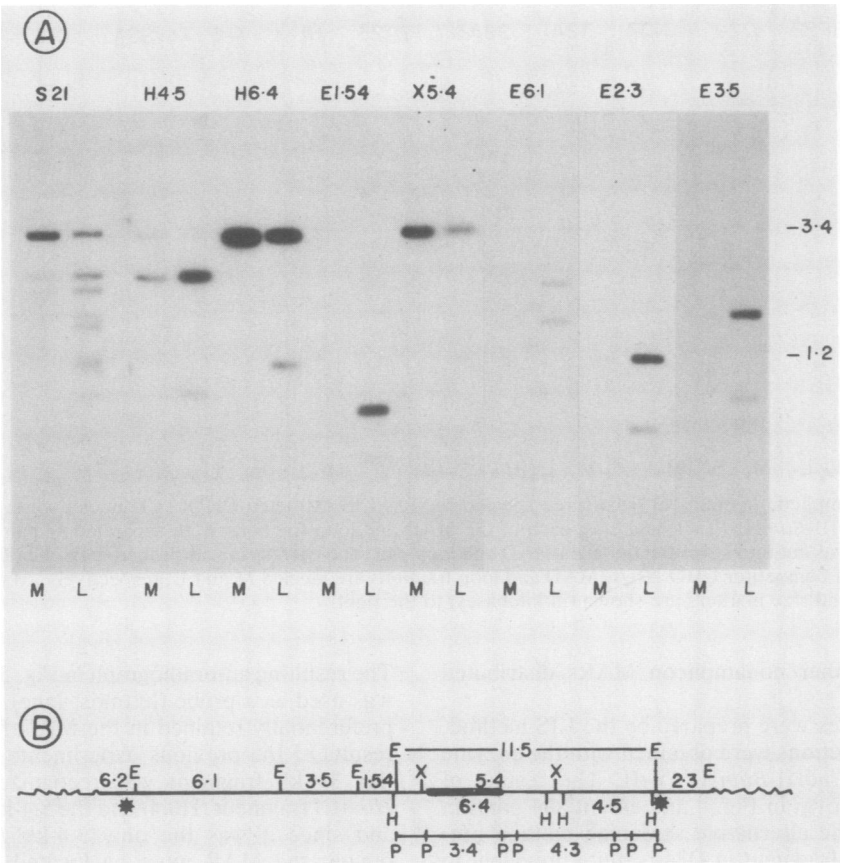

FIG. 5. A specific MAR is found in the region mapping between the two replication initiation sites. (A) LIS matrix-halo structures were isolated from CHOC 400 cells, and the MAD and loop fractions were prepared by digestion with the combination *Eco*RI-*Hin*dIII-*Bam*HI-*Pvu*II. Individual strips of a transfer containing a MAD and loop pair (1 μg each) were probed either with one of several fragments isolated from the cosmid S21 or with the whole cosmid. The MAD and loop fractions are indicated below as M and L, respectively. (B) Map of this region. The sizes of the relevant *Eco*RI fragments are indicated above the scale (note that the single *Xba*I fragment shown is 5.4 kb in length), and the relevant *Hin*dIII fragments are shown below the scale. Note also that *Xba*I and *Pvu*II sites are shown only in the region of the 11.5-kb *Eco*RI fragment. The asterisks indicate the approximate locations of the two replication initiation sites in this locus, and the solid bar on the linear axis indicates the position of the MAR-containing 3.4-kb *Pvu*II fragment.

enzymes and since a 5.2-fold enrichment of the 3.4-kb *Pvu*II fragment was observed in the MAD fraction relative to total genomic DNA (Fig. 5A), we estimate that only 10 to 15% of the amplicons remain attached to the matrix at this sequence during the isolation and enzyme digestion procedures. Thus, by this experimental approach, only a minority of the amplicons in CHOC 400 appear to be bound to the matrix in the vicinity of the replication initiation sites.

However, when the same experiment was performed on matrix-halo structures isolated from parental CHO cells that contain only two copies of this domain per cell (Fig. 7), it could be seen that the 3.4-kb *Pvu*II fragment is markedly more enriched in the MAD fraction of CHO cells than it is in CHOC 400. When the two lanes in the autoradiogram in Fig. 7 were scanned with a densitometer, the signal from the 3.4-kb fragment in the MAD fraction was estimated to be at least 20-fold greater on a weight-per-weight basis than it was in the loop DNA (this is an underestimate, since the signal from the MAD fraction saturated the film at all exposures that allowed detection of the signal in the loop DNA). In parental CHO cells, sequence-specific attachment of the 3.4-kb *Pvu*II fragment to the matrix therefore occurred in close to 50% of the DHFR domains. Since we cannot rule out some destabilization of attachment sites during isolation and

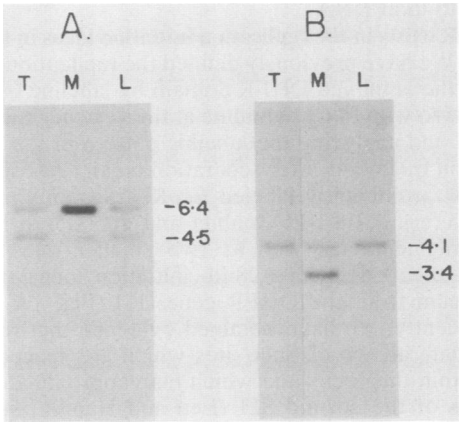

FIG. 6. The MAR in the replication initiation locus can be localized to a 3.4-kb *Pvu*II fragment. LIS matrix-halo structures from CHOC 400 cells were digested with either *Eco*RI and *Hin*dIII (A) or *Eco*RI and *Pvu*II (B). Equal amounts (1 μg) of total DNA (T), MAD (M), and loop DNA (L) were separated on an agarose gel, and after transfer to a membrane were probed with the 11.5-kb *Eco*RI fragment from the initiation locus (Fig. 5B).

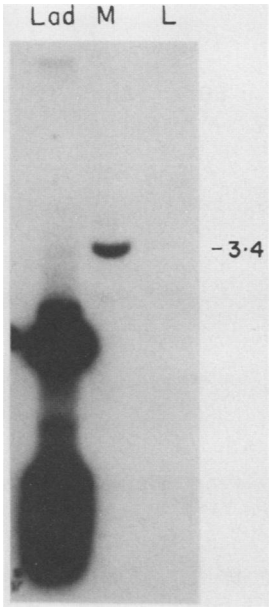

FIG. 7. The MAR in the initiation locus is also detected in parental CHO cells. LIS-extracted matrix-halo structures from parental CHO cells were digested with the combination *Eco*RI-*Hin*dIII-*Bam*HI-*Pvu*II, and 10 μg each of the MAD (M) and loop (L) fractions were separated, along with a 1-kb ladder (Lad) (Bethesda Research Laboratories). After transfer, the digests were probed with the 11.5-kb *Eco*RI fragment from the initiation locus (Fig. 5B). The number on the right indicates kilobases.

digestion protocols, the actual value in the cell could approach 100%.

The 5′-flanking region of the DHFR gene is also attached to the matrix. The data from previous experiments (Fig. 2A, 3B, and 4) suggested that several fragments in the cosmid HDZ23 are somewhat enriched in the MAD fraction in CHOC 400 cells. HDZ23 contains the 5′ half of the DHFR gene and flanking sequences, in addition to the head-to-head junction between the type II amplicons (Fig. 1A). These sequences were mapped with more precision by analyzing the MAD and loop fractions obtained after digestion of LIS matrix-halo structures with the enzyme combination *Eco*RI-*Hin*dIII-*Bam*HI-*Pvu*II. Each of the *Eco*RI fragments in the cosmid HDZ23 was then used to probe a transfer containing equal amounts by weight of the MAD and loop fractions (note that the *Eco*RI fragment used as the probe will hybridize to more than one band in the MAD and loop fractions if it contains an internal recognition sequence for any of the other three enzymes).

Several fragments from this region showed a modest enrichment in the MAD fraction (Fig. 8A). One of these (E4) actually contained the head-to-head junction between the type II amplicons. However, the 4.6-kb E3a probe detected a band approximately 2.8 kb in length that was 3.9-fold more intense in the MAD fraction than it was in the loop DNA. As indicated by the black bar in the map in Fig. 8B, the 4.6-kb E3a *Eco*RI band lies just upstream from the transcription start site for the DHFR gene (which lies in fragment E9). Interestingly, we have previously shown that this 4.6-kb fragment contains a prominent DNaseI-hypersensitive site (1). The data in Fig. 8 therefore show that while several fragments from the region mapping 5′ to the DHFR gene appear to be somewhat enriched in the matrix fraction, the binding is much less localized relative to the MAR detected in the replication initiation locus.

Some, but not all, MARs bind to the nuclear matrix in vitro. In a recently developed in vitro binding procedure (7, 12), isolated nuclear matrices are incubated with a mixture of cloned DNA fragments from a genomic region of interest in order to determine whether any sequences in the mixture bind specifically to the nuclear matrix. In general, sequences that bind specifically to the matrix under these in vitro conditions correspond to those found to be matrix associated by the assays used in the experiments presented in Fig. 4 to 8 (7, 12, 19).

In the experiment shown in Fig. 9A, matrix-halo structures were isolated from parental, drug-sensitive CHO cells, and individual samples of this preparation were each incubated with the restriction enzyme *Hin*dIII in the presence of 1 of the 10 cosmids from the amplicon. Any sequence in a cosmid with affinity for the matrix should therefore bind during the restriction enzyme digestion period (12, 19). After the MAD fraction was purified, it was probed with the corresponding radiolabeled cosmid. (Note that the cosmids were predigested with *Hin*dIII before they were added to the incubation mixture; however, the same results would be obtained with undigested cosmids [not shown]).

The results of this in vitro binding assay are shown in Fig. 9A, and are rather similar, but not identical, to those obtained by the more conventional approaches described in the previous experiments. For example, a MAR was detected in the same 6.4-kb *Hin*dIII fragment from the initiation locus in cosmid S21 that was shown to contain a MAR by the method depicted in Fig. 5A. In addition, in the region spanning the 5′-flanking region of the DHFR gene (HDZ23 and 26A31), several fragments exhibited affinity for the nuclear matrix, as was observed in the experiments shown in Fig. 2, 3, 4, and 8. Among these is a 4.8-kb *Hin*dIII fragment shared by HDZ23 and 26A31 that maps upstream from the promoter region of the DHFR gene and overlaps the 4.6-kb *Eco*RI fragment that was observed to be enriched in the MAD fraction in Fig. 8A.

However, no fragments from the cosmid O24 were specifically absorbed to the matrix during the in vitro binding assay (Fig. 9A); in addition, several bands in the cosmid Q23 were seen to have a modest affinity for the matrix during the in vitro incubation reaction, but these fragments were not detected by other methods. Finally, the in vitro binding assay detected a 3.4-kb *Hin*dIII fragment in cosmid PA36 that had a high affinity for the matrix but which was not detected by any other approach. From the results of preliminary mapping studies, this fragment appears to be located within ~5 kb of the junction between the type 1 amplicons in CHOC 400 (data not shown), but we have not yet characterized this fragment in detail.

DISCUSSION

The aim of the present study was to determine the distribution of matrix attachment sites relative to functional elements within the DHFR domain. By two different methods of analysis, we identified a MAR that maps in the replication initiation locus. Binding to the matrix also occurs in the 5′-flanking region of the DHFR gene, albeit in a much less localized fashion. The MAR identified in the region represented by cosmid O24 cannot presently be associated geographically with a functional element, since no transcripts, origins, or interamplicon junctions have been mapped to this locus. An in vitro binding assay also detected

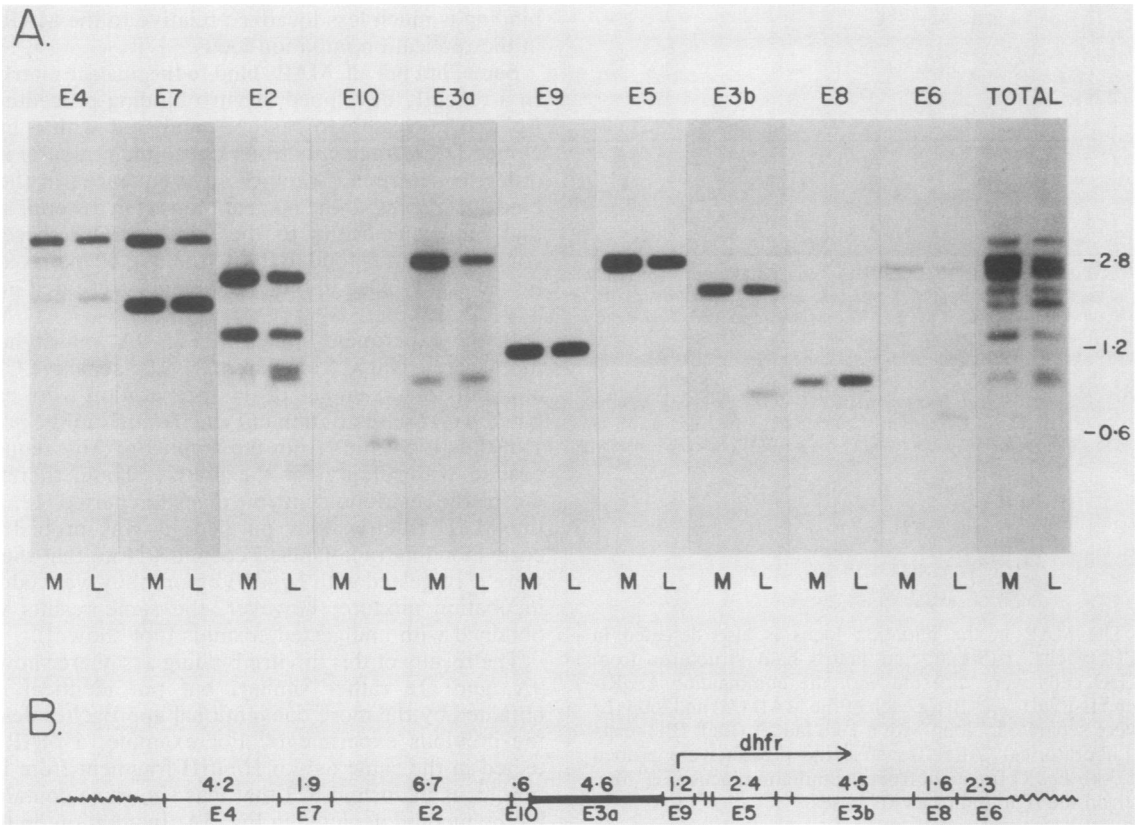

FIG. 8. An extensive region upstream from the DHFR gene is associated with the nuclear matrix. (A) The MAD and loop fractions from LIS-extracted CHOC 400 nuclei were obtained by digestion with the combination *Eco*RI-*Hin*dIII-*Bam*HI-*Pvu*II, and 1 μg each of MAD (M) and loop (L) DNA were separated, transferred, and probed with each of the *Eco*RI fragments from the cosmid HDZ23, which contains the 5′ half of the DHFR gene and flanking sequences. The rightmost lane (TOTAL) was probed with the whole cosmid HDZ23. Size markers (in kilobases) are indicated to the right. (B) The sizes of the *Eco*RI fragments in this region are shown. The 4.6-kb MAR-containing fragment is indicated by the solid bar on the scale, and the direction of transcription is indicated by the arrow.

a MAR near the junction between the type 1 amplicons but failed to detect the MAR in O24. Thus, our data show that MARs are distributed nonrandomly with respect to DNA sequence in the DHFR amplicons and further suggest that at least some of these matrix attachment sites are located near functional sequence elements in the genome. However, our data also show that different methods of defining MARs may give a somewhat different spectrum of matrix-attached sequences.

The presence of a MAR in the region between the two replication initiation sites is an interesting finding that will not be fully appreciated until we have characterized these sites further. If the two initiation sites turn out to be true origins that are independent of one another, our data would suggest that the MAR may actually represent a terminus of replication. The replication of the region midway between these two initiation sites appears to be delayed beyond the time expected based on the rate of replication fork travel in mammalian cells (Leu and Hamlin, submitted). This could be due in part to the buildup of torsional stress and the complex events that must follow to relieve that stress and separate chromatids (34). It is also conceivable, however, that the replication of this region is delayed in order to hold the two daughter chromatids together along their length until the time of chromatid separation prior to mitosis, and the MAR could represent the place at which replication forks are stopped or slowed. It will be interesting to determine whether the MAR that we have identified in this region is a preferred topoisomerase II cutting site (31), since this enzyme must be involved in the complex resolution events that would occur in this region according to this model.

Alternatively, the two initiation sites identified in this region may actually constitute a single, complex origin, of which the MAR represents a critical functional component. While unorthodox, this proposal is most compatible with the results of autoradiographic studies on matrix-halo structures prepared from synchronized cells (10). After a brief pulse with [^{3}H]thymidine at the beginning of S phase (when initiation at origins is occurring), silver grains were shown to be concentrated over the central matrix and to remain so even after a chase with cold thymidine. In contrast, label administrated later in S phase migrated into the peripheral DNA halo during the chase period (10). From this it was inferred that both initiation and elongation events occur on the matrix through the agency of a replication complex but that the origin remains associated permanently with the matrix during the cell cycle (10). This model could be extended to suggest that torsional stress is relieved by the continual action of topoisomerase II on a specific site in the MAR during replication of a loop.

The finding of a MAR in the 5′-flanking region of the DHFR gene is in good agreement with previous reports in which MARs have been shown to occur in the sequences immediately upstream from several active genes, usually close to enhancerlike elements (12). However, our results are different than those obtained by Kas and Chasin on an

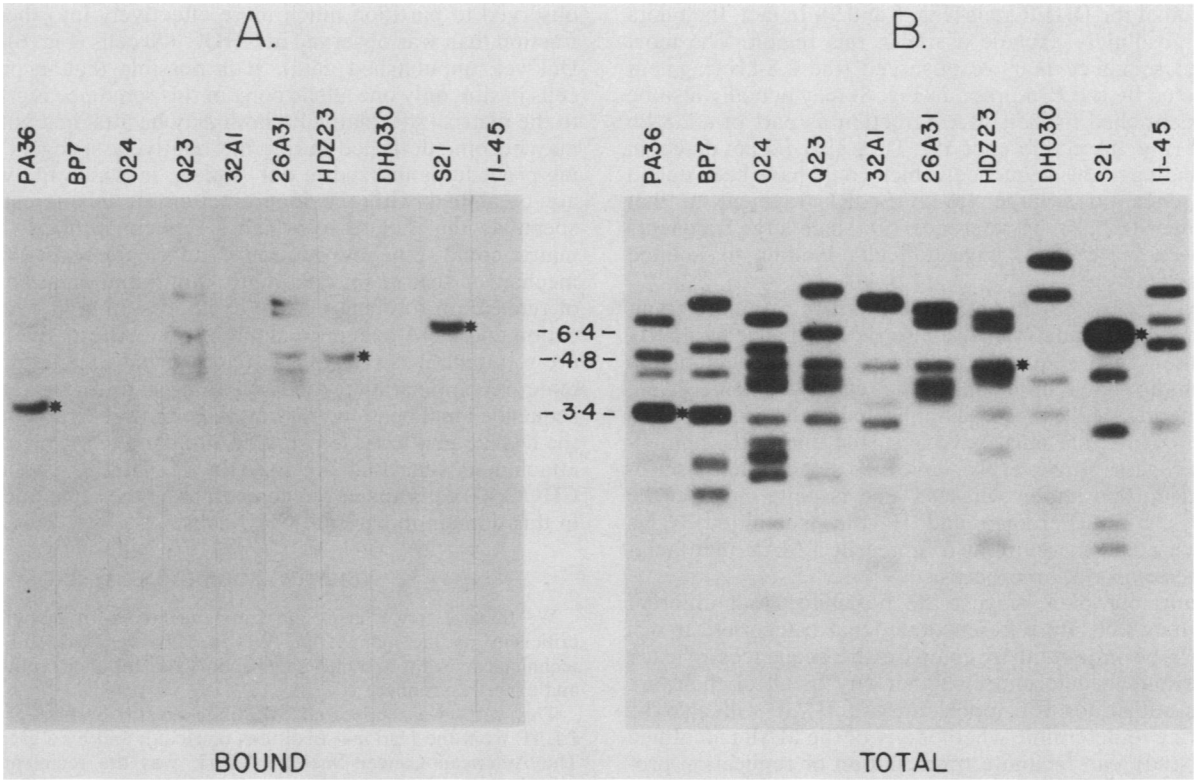

FIG. 9. An in vitro binding assay detects a similar, but not identical, spectrum of MARs in the DHFR amplicon. (A) Nuclear matrix-halo structures were prepared from parental CHO cells by the LIS extraction method, and the DNA loops were removed from the matrices with *Hin*dIII in the presence of a *Hin*dIII digest of each one of the indicated cosmids (see Materials and Methods). After a 3-h digestion, the matrix-cosmid mixtures were washed and the MAD fraction from each was purified. After separation of samples on a gel and transfer to a membrane, each sample was probed with the corresponding cosmid in order to illuminate selective retention of particular fragments from the cosmid by the matrix. The three most prominent MARs are indicated with asterisks. (B) Each of the cosmids used in panel A was digested with *Hin*dIII; after separation and transfer the transfer was cut into strips, and each strip was probed with the corresponding cosmid. The resulting patterns represent the spectrum of fragments that were presented to the CHO matrix during the in vitro binding reaction. Note that the cosmid S21 contains a triplet that includes a 6.4-kb pHC79 vector monomer plus two genomic *Hin*dIII fragments that are 6.4 and 6.75 kb in length. The 6.4-kb fragment that is selectively bound to the matrix is assumed to be the genomic fragment. The sizes (in kilobases) of the most prominent MARs are indicated.

independently isolated methotrexate-resistant CHO cell line, UK3 (19). These authors did not identify the MAR mapping upstream from the DHFR gene but detected two separate MARs in the neighborhood of the fourth exon.

There are several possible reasons for this discrepancy. It is conceivable, of course, that the two methotrexate-resistant CHO cell lines, CHOC 400 and UK3, actually utilize different MARs to affix the same DNA sequence to the nuclear matrix. However, Kas and Chasin found the same two intragenic MARs in several other Chinese hamster cell lines, including parental CHO cells (19), and we have shown that at least the MARs identified in cosmids S21 and HDZ23 are also detectable in CHO cells (Fig. 7) (P. A. Dijkwel, unpublished observations). Although these findings argue against gross differences among cell lines, there remains the possibility that the CHOC 400 and UK3 cell lines differ in critical regions of the amplicon. For example, we did not detect enrichment in the MAD fraction of either the 1.8-kb *Hin*dIII fragment from intron 4 or the 3.0-kb *Eco*RI fragment that spans this intron, even though these fragments contain the two MARs described by Kas and Chasin (19). Rather, we observed modest enrichment of several fragments mapping upstream from the body of the DHFR gene. This suggests that attachment of genomic DNA to the matrix in this region of the amplicon differs from that observed in the replication initiation locus, in which a single MAR was detected. The observed differences in our two studies could be the consequence of the head-to-head arrangement of the predominating type II amplicons in the CHOC 400 cell line (22, 24). Because of this arrangement, the 5′ ends of two adjacent DHFR genes are in close proximity to one another (Fig. 1). Moreover, an interamplicon junction is present halfway between the two 5′ ends of the type II amplicon. Consequently, it could be argued that this particular arrangement, which appears to be unique to CHOC 400 cells (23), facilitates occurrence of MARs in this region of the amplicon and frees the cell of the necessity to anchor the DHFR gene to the matrix intragenically.

Differences in the method of matrix preparation may also underlie some of the differences in our two studies. For example, our LIS extraction procedure involves two treatments with LIS, and digestion of this fraction with a single enzyme, such as *Eco*RI, yields a MAD fraction that contains only 4% of the genomic DNA. In contrast, the MAD fractions of Kas and Chasin contain 20 to 25% residual DNA (19). The apparently greater stringency of our method could therefore account for the failure to detect the intragenic MARs that they observed in the fourth intron of the DHFR gene. However, this does not explain why Kas and Chasin did not detect the MARs that we observed upstream from

the 5′ end of the DHFR gene (Fig. 8 and 9). In fact, their data do not absolutely exclude a site in this region. The most enriched sequence that we observed (the 2.8-kb fragment illuminated by the E3a probe in Fig. 8) may actually also be slightly enriched in their MAD fraction as part of a 2.8-kb doublet (Fig. 2A in reference 19). They also did not detect in vitro binding of this sequence, which could have been due to its presence on a large 4.6-kb *Eco*RI fragment in that experiment (Fig. 4A in reference 19), since large fragments have been reported to have difficulty binding to isolated matrices (18).

In the in vitro binding assay (but not in the more traditional method of analysis), we also detected specific matrix association of a sequence mapping close to the junction between the type I amplicons in the region of cosmid PA36. This potential MAR could be implicated in the breakage and reunion events that must have occurred during the amplification process. However, we have also detected a transcription unit in this region whose 5′ end is quite close to the actual junction (Foreman and Hamlin, submitted). This sequence could therefore also represent a MAR that facilitates the transcription process.

In sum, our data suggest the possibility that different MARs may fall into different functional categories. It will therefore be important to compare the sequences of each element and to determine whether any or all of them are specific substrates for topoisomerase II. It will also be interesting to determine whether any of the MARs identified in this study can facilitate transcription or replication processes of cloned reporter genes or origins, such as would be expected of an enhancer.

The occurrence of MARs at 70- to 120-kb intervals within the DHFR locus agrees well with estimates for the average size of DNA loops in mammalian cells (6, 21, 34). In several studies, it has been suggested that chromosomal loops correspond to replicons on the basis of their similar average sizes and proposed mechanisms for DNA replication (e.g., 6, 34). However, as shown in the map of the type I amplicon in Fig. 1A (which essentially corresponds to the parental DHFR locus), the loop defined by the MARs in O24 and HDZ23 contains no replication initiation site. This loop is therefore, by definition, smaller than a replicon.

None of the potential MARs identified in this study appear to be attached to the matrix in more than ~20% of the amplicons in the CHOC 400 cell line. It is possible that some MARs are only transiently associated with the matrix during the cell cycle (e.g., to facilitate replication initiation or during transcription), so that in a log-phase population (as was used in this study), only a subset of the MARs partition to the MAD fraction. However, when matrices were isolated from cells collected at the G1/S boundry with aphidicolin, the percent attachment of any given MAR was not markedly different than those described in this report (data not shown). The caveat is that replication initiation could have already occurred in cells arrested with aphidicolin or that the drug somehow might weaken the interaction of MARs with the scaffold.

It is also possible that the concentration of attachment sites is not high enough to accommodate the attachment of 1,000 additional copies of the amplified domain in a localized region of the nucleus or that the extra copies are attached less strongly and are dissociated during the preparation and washing procedures. When matrix-halo structures were prepared from parental CHO cells, both the 3.4-kb *Pvu*II sequence located between the two initiation sites and the 4.6-kb *Eco*RI fragment upstream from the DHFR gene were observed to partition much more effectively into the MAD fraction than was observed in CHOC 400 cells (Fig. 6) (P. A. Dijkwel, unpublished data). It is possible that in parental cells in situ, only one allelic copy of this sequence is attached to the matrix. Alternatively, both may be attached but some may become detached during the relatively stringent washing procedures utilized in our studies, in which the washes are combined with the loop fraction. It is interesting to speculate that failure to attach a replicon properly to the matrix could somehow neutralize a normal negative control mechanism that might operate to limit initiation at an origin of replication to once per cell cycle, resulting in overreplication and DNA sequence amplification. Alternatively, failure to attach properly to the matrix could facilitate illegitimate recombination processes that lead to or facilitate sequence amplification. However, even though all copies of the DHFR amplicons may not be atttached to the matrix, the attachment sites that are used in the DHFR amplicon in CHOC 400 cells appear, in general, to be the same ones used in this domain in parental CHO cells.

ACKNOWLEDGMENTS

We thank Larry Chasin and Emmanuel Kas for many helpful criticisms on the manuscript. We are also very grateful to our technicians, Carlton White and Kevin Cox, for their enthusiastic and expert assistance.

This work was supported by Public Health Service grants to J.L.H. from the National Institutes of Health and by a grant from The American Cancer Society. J.L.H. was the recipient of an American Cancer Society Faculty Research Award.

LITERATURE CITED

1. **Azizkhan, J. C., J. P. Vaughn, R. J. Christy, and J. L. Hamlin.** 1986. Nucleotide sequence and nuclease hypersensitivity of the Chinese hamster dihydrofolate reductase gene promoter region. Biochemistry **25**:6228–6236.
2. **Bekers, A. G. M., H. J. Gijzen, R. D. F. Taalman, and F. Wanka.** 1981. Ultrastructure of the nuclear matrix from *Physarum polycephalum* during the mitotic cycle. J. Ultrastruct. Res. **75**:352–362.
3. **Berezney, R., and D. S. Coffey.** 1974. Identification of a nuclear protein matrix. Biochem. Biophys. Res. Commun. **60**: 1410–1417.
4. **Berezney, R., and D. S. Coffey.** 1975. Nuclear protein matrix: association with newly synthesized DNA. Science **189**:291–293.
5. **Berrios, M., N. Osheroff, and P. Fisher.** 1985. *In situ* localization of DNA topoisomerase II, a major polypeptide component of the *Drosophila* nuclear matrix. Proc. Natl. Acad. Sci. USA **83**:4142–4146.
6. **Buongiorno-Nardelli, M., G. Micheli, M. T. Carri, and M. Marilley.** 1982. A relationship between replicon size and supercoiled loop domains in the eucaryotic genome. Nature (London) **298**:100–102.
7. **Cockerill, P. N., and W. T. Garrard.** 1986. Chromosomal loop anchorage of the kappa immunoglobulin gene occurs next to the enhancer in a region containing topoisomerase II sites. Cell **44**:273–282.
8. **Cook, P. R., and I. A. Brazell.** 1976. Conformational constraints in nuclear DNA. J. Cell Sci. **22**:287–302.
9. **Dijkwel, P. A., L. H. F. Mullenders, and F. Wanka.** 1979. Analysis of the attachment of replicating DNA to a nuclear matrix in mammalian interphase nuclei. Nucleic Acids Res. **6**:219–230.
10. **Dijkwel, P. A., P. W. Wenink, and J. Poddighe.** 1986. Permanent attachment of replication origins to the nuclear matrix in BHK cells. Nucleic Acids Res. **14**:3241–3249.
11. **Feinberg, A. P., and B. Vogelstein.** 1983. High specific activity labeling of DNA restriction endonuclease fragments. Anal. Biochem. **132**:6–13.
12. **Gasser, S. M., and U. K. Laemmli.** 1986. Cohabitation of

scaffold binding regions with upstream enhancer elements of three developmentally-regulated genes of *D. melanogaster*. Cell **46**:521–530.
13. **Gasser, S. M., and U. K. Laemmli.** 1986. The organization of chromatin loops: characterization of a scaffold attachment site. EMBO J. **5**:511–518.
14. **Gasser, S. M., T. Laroche, J. Falquet, E. Boy de la Tour, and U. K. Laemmli.** 1986. Metaphase chromosome structure. Involvement of topoisomerase II. J. Mol. Biol. **188**:613–629.
15. **Hamlin, J. L., J. D. Milbrandt, N. H. Heintz, and J. C. Azizkhan.** 1984. DNA sequence amplification in mammalian cells. Int. Rev. Cytol. **90**:31–82.
16. **Heintz, H. H., and J. L. Hamlin.** 1982. An amplified chromosomal sequence that includes the gene for dihydrofolate reductase initiates replication within specific restriction fragments. Proc. Natl. Acad. Sci. USA **69**:4083–4087.
17. **Heintz, N. H., J. D. Milbrandt, K. S. Greisen, and J. L. Hamlin.** 1983. Cloning the initiation region of a mammalian chromosomal replicon. Nature (London) **302**:439–441.
18. **Izaurralde, J. Mirkovitch, and U. K. Laemmli.** 1988. Interaction of DNA with nuclear scaffolds *in vitro*. J. Mol. Biol. **200**: 111–125.
19. **Kas, E., and L. A. Chasin.** 1987. Anchorage of the Chinese hamster dihydrofolate reductase gene to the nuclear scaffold occurs in an intragenic region. J. Mol. Biol. **198**:677–692.
20. **Labarca, C., and K. Paigen.** 1980. A simple, rapid and sensitive DNA essay procedure. Anal. Biochem. **102**:344–352.
21. **Linskens, M. H. K., A. Eijsermans, and P. A. Dijkwel.** 1987. Comparative analysis of DNA loop length in nontransformed and transformed hamster cells. Mutat. Res. **178**:245–256.
22. **Looney, J. E., and J. L. Hamlin.** 1987. Isolation of the amplified dihydrofolate reductase domain from methotrexate-resistant Chinese hamster ovary cells. Mol. Cell. Biol. **7**:569–577.
23. **Looney, J. E., C. Ma, T.-H. Leu, W. F. Flintoff, W. B. Troutman, and J. L. Hamlin.** 1988. The dihydrofolate reductase amplicons in different methotrexate-resistant Chinese hamster cell lines share at least a 273-kilobase core sequence, but the amplicons in some cell lines are much larger and are remarkably uniform in structure. Mol. Cell. Biol. **8**:5268–5279.
24. **Ma, C., J. E. Looney, T.-H. Leu, and J. L. Hamlin.** 1988. Organization and genesis of dihydrofolate reductase amplicons in the genome of a methotrexate-resistant Chinese hamster ovary cell line. Mol. Cell. Biol. **8**:2316–2327.
25. **Milbrandt, J. D., N. H. Heintz, W. C. White, S. M. Rothman, and J. L. Hamlin.** 1981. Methotrexate-resistant Chinese hamster ovary cells have amplified a 135 kilobase pair region that includes the dihydrofolate reductase gene. Proc. Natl. Acad. Sci. USA **78**:6043–6047.
26. **Mirkovitch, J., M.-E. Mireault, and U. K. Laemmli.** 1984. Organization of the higher order chromatin loop: specific DNA attachment sites on the nuclear scaffold. Cell **39**:223–232.
27. **Mitchell, P. J., A. M. Carothers, J. H. Han, J. D. Harding, E. Kas, L. Venolia, and L. A. Chasin.** 1986. Multiple transcription start sites, DNAse I hypersensitive sites, and an opposite strand exon in the 5′ region of the CHO dihydrofolate reductase gene. Mol. Cell. Biol. **6**:425:440.
28. **Montoya-Zavala, M., and J. L. Hamlin.** 1985. Similar 150-kilobase DNA sequences are amplified in independently-derived methotrexate-resistant Chinese hamster cells. Mol Cell. Biol. **5**:619–627.
29. **Paulson, J., and U. K. Laemmli.** 1977. The structure of histone-depleted metaphase chromosomes. Cell **12**:817–828.
30. **Razin, S. V., M. G. Kekelidze, E. M. Lukanidin, K. Scherrer, and G. P. Georgiev.** 1986. Replication origins are attached to the nuclear skeleton. Nucleic Acids Res. **14**:8189–8207.
31. **Sander, M., and T. Hsieh.** 1985. *Drosophila* topoisomerase II double-strand DNA cleavage: analysis of DNA sequence homology at the cleavage site. Nucleic Acids Res. **13**:1057–1071.
32. **Schimke, R. T.** 1984. Gene amplification in cultured animal cells. Cell **37**:705–713.
33. **Small, D., B. Nelkin, and B. Vogelstein.** 1985. The association of transcribed genes with the nuclear matrix of *Drosophila* cells during heatshock. Nucleic Acids Res. **13**:2413–2431.
34. **Sundin, O., and A. Varshavsky.** 1980. Terminal stages of SV40 DNA replication proceed via multiply intertwined catenated dimers. Cell **21**:103–114.
35. **Van der Velden, H. M. W., G. van Willigen, R. H. W. Wetzels, and F. Wanka.** 1984. Attachment of origins of replication to the nuclear matrix and chromosomal scaffold. FEBS Lett. **161**: 13–16.
36. **Vogelstein, B., D. M. Pardoll, and D. S. Coffey.** 1980. Supercoiled loops and eukaryotic DNA replication. Cell **22**:79–85.